

Break up of the heavy electron at a quantum critical point

J. Custers*, P. Gegenwart*, H. Wilhelm*, K. Neumaier†, Y. Tokiwa*, O. Trovarelli*, C.

Geibel*, F. Steglich*, C. Pépin‡ & P. Coleman§

**Max-Planck-Institute for the Chemical Physics of Solids, D-01187 Dresden, Germany*

*†Walther-Meissner-Institute for Low Temperature Research of the Bavarian Academy of Sciences,
D-85748 Garching, Germany*

‡SPHT, L'Orme des Merisiers, CEA-Saclay, 91190 Gif-sur-Yvette, France

*§CMT, Department of Physics and Astronomy, Rutgers University, Piscataway, NJ 08854-8019,
USA*

(January 27, 2018)

The point at absolute zero where matter becomes unstable to new forms of order is called a quantum critical point (QCP). The quantum fluctuations between order and disorder¹⁻⁵ that develop at this point induce profound transformations in the finite temperature electronic properties of the material. Magnetic fields are ideal for tuning a material as close as possible to a QCP, where the most intense effects of criticality can be studied. A previous study⁶ on the heavy-electron material $YbRh_2Si_2$ found that near a field-induced quantum critical point electrons move ever more slowly and scatter off one-another with ever increasing probability, as indicated by a divergence to infinity of the electron effective mass and cross-section. These studies could not shed light on whether these properties were an artifact of the applied field^{7,8}, or a more general feature of field-free QCPs. Here we report that when Germanium-doped $YbRh_2Si_2$ is tuned away from a chemically induced quantum critical point by magnetic fields there is a universal behavior in the temperature dependence of the specific heat and resistivity: the characteristic kinetic energy of electrons is directly proportional to the strength of the applied field. We infer that all ballistic motion of electrons vanishes at a QCP, forming a new class of conductor in which individual

electrons decay into collective current carrying motions of the electron fluid.

Recent work⁶ on the heavy electron material YbRh_2Si_2 ⁹ has demonstrated that a magnetic field can be used to probe the heavy electron quantum critical point. This material exhibits a small antiferromagnetic (AFM) ordering temperature $T_N = 70$ mK (Fig. 1a) that is driven to zero by a critical magnetic field $B_c = 0.66$ T (if the field is applied parallel to the crystallographic c -axis, perpendicular to the easy magnetic plane)⁶. For $B > B_c$, a field-induced Landau Fermi Liquid (LFL) state characterized by $\Delta\rho = AT^2$ (where $\Delta\rho(T) = \rho(T) - \rho_o$ is the temperature dependent part of the electrical resistivity) is established below some cross-over temperature $T_0(B)$ which grows linearly with field. The A coefficient, being proportional to the quasiparticle-quasiparticle scattering cross section was found to diverge as $A(B) \propto 1/(B - B_c)$ for $B \rightarrow B_c$. Comparative studies of the resistivity and the electronic specific heat $C_{el}(T) = \gamma_o(B)T$ in the field ranges 0.5 T – 4 T ($B \perp c$ with $B_c = 0.06$ T) and 2 T – 6 T ($B \parallel c$) revealed a field-independent ratio A/γ_0^2 slightly smaller than the empirical Kadowaki-Woods ratio¹³ that holds for LFL systems. This seemed to suggest a divergence of the effective quasiparticle (QP) mass as $1/(B - B_c)^{1/2}$ as $B \rightarrow B_c$. In this letter, we report the first-ever observation of the divergence of the QP mass at a QCP, established very close to $B = 0$.

By alloying YbRh_2Si_2 with Germanium, using a nominal concentration $x = 0.05$, we have been able to fine-tune, in a new set of studies, the Néel temperature of this material and the critical field far closer to zero, to a point where, for the first time, we may reliably probe the zero-field transition using field-tuning. The phase diagram for a high-quality $\text{YbRh}_2(\text{Si}_{0.95}\text{Ge}_{0.05})_2$ single crystal is shown in Fig. 1b. NFL behavior dominates over a funnel-shaped region of the T - B phase diagram down to the lowest accessible temperature of 20 mK. The critical field has been suppressed to as low as $B_c = 0.027$ T ($B \perp c$). As in the undoped material, there is a broad cross-over regime between the NFL and field polarized LFL regime with a mean cross-over temperature T_o that is seen to rise linearly with the field B . Very weak AFM order develops in the $x = 0.05$ sample below $T_N = 20$ mK, as evidenced by the extremely weak anomaly in the electronic specific heat coefficient (Fig. 2a).

Past experience^{7,8} suggested that a finite field quantum critical point has properties which are qualitatively different to a zero field transition, shedding doubt on the reliability of these measurements as an indicator of the physics of a quantum phase transition at zero field. However, the zero-field properties of $\text{YbRh}_2(\text{Si}_{1-x}\text{Ge}_x)_2$ above $T \approx 70$ mK for the undoped ($x = 0$) and doped ($x = 0.05$) crystals are essentially identical (Fig. 2a), suggesting that by suppressing the critical field we are still probing the same quantum critical point. In both compounds, the ac-susceptibility follows a temperature dependence $\chi^{-1} \propto T^\alpha$ from 0.3 K to $\leq T \leq 1.5$ K, with $\alpha = 0.75$ ¹⁴, and the coefficient of the electronic specific heat, $C_{\text{el}}(T)/T$, exhibits⁹ a logarithmic divergence between 0.3 K and 10 K. However, in the low- T paramagnetic regime, i. e., $T_{\text{N}} < T \lesssim 0.3$ K, the ac-susceptibility follows a Curie-Weiss law (inset of Fig. 2a) with a Weiss temperature $\Theta_{\text{W}} \approx 0.3$ K, and a surprisingly large effective moment $\mu_{\text{eff}} \approx 1.4\mu_{\text{B}}/\text{Yb}^{3+}$, indicating the emergence of coupled, unquenched spins at the quantum critical point. The electronic specific heat coefficient, $C_{\text{el}}(T)/T$, exhibits a pronounced upturn below 0.3 K (Fig. 2a).

We now discuss the field dependence of the electronic specific heat in $\text{YbRh}_2(\text{Si}_{0.95}\text{Ge}_{0.05})_2$ in more detail. In these measurements, magnetic fields were applied perpendicular to the crystallographic c -axis, within the easy magnetic plane (Fig. 2b). At fields above 0.1 T, C_{el}/T is weakly temperature independent, as expected in a LFL¹⁵. A weak maximum is observed in $C_{\text{el}}(T)/T$ at a characteristic temperature $T_o(B)$ which grows linearly with the field (inset of Fig. 3a), indicating that entropy is transferred from the low-temperature upturn to higher temperatures by the application of a field $B \geq B_c = 0.027$ T. As the field is lowered the temperature window over which $C_{\text{el}}(T, B)/T = \gamma_o(B)$ is constant shrinks towards zero and the zero-temperature $\gamma_o(B)$ diverges (Fig. 3a). For example, in a field of 0.05 T a constant value $\gamma_o(B) \approx 1.54(7)$ Jmol⁻¹K⁻² only develops below 40 mK. These results indicate the formation of a field-induced LFL state at a characteristic scale $T \lesssim T_o(B)$. As the window of LFL behavior is reduced towards zero, an ever increasing component of the zero-field upturn in the specific heat coefficient is revealed in the temperature dependence. This confirms that the major part of the upturn in the specific heat coefficient observed in zero field is electronic

in character, and must be associated with the intrinsic specific heat at the QCP.

This conclusion is also supported by the electrical resistivity data which reveal a field-dependent cross-over from a T -linear resistivity at high temperatures, to quadratic behavior $\Delta\rho = A(B)T^2$ at sufficiently low temperatures. Most importantly, the data show that at low fields and temperatures, the same scale $T_o(b) \propto b$ (where $b = B - B_c$ is the deviation from the critical field) governs the cross-over from LFL to NFL behavior in *both* the thermodynamics *and* the resistivity. This can be quantitatively demonstrated by noting that the finite field transport and specific heat data collapse into a single set of scaling relations (see Fig. 3 inserts),

$$\frac{C_V}{T} = \frac{1}{b^{1/3}}\Phi\left(\frac{T}{T_o(b)}\right), \quad \frac{d\rho}{dT} = F\left(\frac{T}{T_o(b)}\right), \quad (1)$$

where $\Phi(x) \sim (\max(x, 1))^{-1/3}$ and $F(x) \sim x/\max(x, 1)$. The NFL physics is described by the $x \rightarrow \infty$ ($T \gg T_o(b)$) behavior of these equations, where $d\rho/dT$ is constant and $C_V/T \propto T^{-1/3}$. By contrast, the field-tuned LFL is described by the $x \rightarrow 0$ limit of these equations. Were there any residual pockets of LFL behavior that were left unaffected by the QCP, we would expect a residual quadratic component in the resistivity, and the data would not collapse in the observed fashion. We are thus led to believe that the break up of the LFL involves the entire Fermi surface.

From the second scaling relation in (1), we see that the A -coefficient of the T^2 term to the resistivity diverges roughly as $1/b$, a result that is consistent with earlier measurements on pure YbRh_2Si_2 carried out further away from the QCP coefficient $\gamma_o(b)$ grows as $b^{-1/3}$ (Fig. 2a). Notice that the field dependence at absolute zero temperature can be interchanged with the temperature dependence at $B = B_c$, but only in the upturn region. At high magnetic field deviations from the QCP, earlier measurements showed⁶ that the Kawasaki Woods ratio¹³ $K = A/\gamma_o^2$ is approximately constant. Closer to the QCP, where the scaling behavior is observed, $K = A/\gamma_o^2 \approx b^{-1/3}$ is found to contain a weak field dependence (Fig. 3b).

We now turn to discuss the broader implications of our measurements. The observed

divergence of both the A -coefficient and the coefficient γ_o of the T -linear specific heat certainly rule out a 3D SDW scenario, which predicts that both quantities will remain finite at sufficiently low temperature in the approach to a zero-field QCP ($B \rightarrow B_c \rightarrow 0$), but it can be used to obtain still more insight into the underlying scattering mechanisms between the quasiparticles. In a 2D SDW scenario, the scattering amplitude between two heavy electrons is severely momentum dependent. When used to compute the transport relaxation rate, the SDW scenario leads to the result $A \propto 1/\kappa^2$, with κ the inverse correlation length¹⁶. The observed divergence in $A(b)$ would require $\kappa^2 \propto b$. However, the fluctuations of the soft 2D spin fluctuations only produce a weak logarithmic renormalization in the heavy electron density of states, measured by the specific heat coefficient, $\gamma_o \propto \ln(1/\kappa)$. Thus the 2D SDW scenario predicts a weak divergence in the in- T linear specific heat, but a strongly field dependent enhancement of the Kadowaki Woods ratio in the approach to a QCP ($b \rightarrow 0$), given by

$$\gamma_{SDW} \propto \ln(1/b) \quad \text{and} \quad K_{SDW} \propto \frac{1}{b \ln^2(b)}. \quad (2)$$

The strong violation of these predictions by our data, presented in Fig. 3a and 3b, rules out 2D spin fluctuations as the driving force behind the thermodynamics and the dominant source of scattering near the heavy electron QCP.

Taking a more general view, scaling behavior of the transport scattering rate tells us that the only scale entering into the density of states and the scattering amplitude is the single scale $T_o \propto b$ of the heavy electron fluid. A truly field-independent Kadowaki Woods ratio would indicate that the quasiparticle scattering amplitude has the form

$$A^* = T_F^* \mathcal{F}[\{k_{in}\} \rightarrow \{k_{out}\}]. \quad (3)$$

The weak field dependence of the Kadowaki Woods ratio over a wide range of fields implies that the characteristic length scale of the most singular scattering amplitudes renormalizes more slowly in the approach to the QCP than expected in a SDW scenario.

Our data also provide some insight into the thermodynamics in the vicinity of the QCP.

By integrating the scaling form (1) for the specific heat over temperature, the entropy $S(T) = \int_0^T dT' (C_V/T')$ in the vicinity of the QCP can be described by the form

$$S(T, B) = b^{1-\eta} \mathcal{S} \left(\frac{T}{T_o(b)} \right) \quad (4)$$

where $\eta = 1/3$. The appearance of a field-dependent pre-factor in this equation forces the entropy to vanish at the QCP, as required by the third law of thermodynamics. The exponent in the pre-factor also determines the effective Fermi temperature $T_F^*(b) \propto \gamma(b)^{-1} \propto T_o(b)^\eta$. Thus the requirement that the entropy vanishes at the QCP ($\eta < 1$) prevents a direct proportionality between the Fermi temperature of the heavy LFL and the scale $T_o(b)$ governing the cross-over to NFL behavior. It follows that the Fermi temperature and cut-off temperature $T_o(b)$ must obey a relationship of the form

$$T_F^*(b) = T_\Lambda \left(\frac{T_o(b)}{T_\Lambda} \right)^\eta \quad (5)$$

where T_Λ is an upper cut-off that we might identify with the single ion Kondo temperature of the Yb^{3+} ions ($\approx 25\text{K}$). Such a power law renormalization of the characteristic energy scale would be expected in the presence of locally critical fluctuations that extend down from T_Λ to the infra-red cut-off provided, in this case, by the magnetic field¹⁷.

In this respect, our results support the conclusions recently drawn from earlier measurements on the quantum critical material $\text{CeCu}_{6-x}\text{Au}_x$ ($x = 0.1$)¹⁸, and used in a recently proposed theory for quantum criticality by Si *et al.*⁴, suggesting that the most critical scattering is neither three, two or even one dimensional, but local– as if the most critical fluctuations in the underlying quantum phase transition are fundamentally “zero dimensional” in character.

One of our most striking observations is that below $T \approx 0.3\text{ K}$ where $\chi(T)$ follows a Curie-Weiss law, the electronic specific heat coefficient $C_{el}(T)/T$ for both samples starts to deviate towards larger values, separating away from the $-\log T$ dependence that is valid⁹ up to 10 K (Fig. 2a). This “upturn” continues in the $x = 0.05$ sample down to approximately 20 mK, if the critical field of 0.027 T ($B \perp c$) is applied. We ascribe this intrinsically electronic feature

to the critical fluctuations associated with the zero-field quantum phase transition that exists at a slightly larger Ge concentration. The unique temperature dependence of $C_{el}(T)/T$ for $T < 0.3$ K is *disparate* from the linear temperature dependence of the electrical resistivity which holds all the way from ≥ 10 K to $T \approx 10$ mK. Since the former (thermodynamic) quantity probes the dominating local $4f$ (“spin”) part of the composite quasiparticles, while the latter (transport) quantity is sensitive to the itinerant conduction-electron (“charge”) part, one may view the observed disparity as a direct manifestation of the *break up* of the composite fermion in the approach to the QCP.

REFERENCES

- ¹ Hertz, J.A., Quantum critical phenomena. *Phys. Rev. B* **14**, 1165-1184 (1976).
- ² Millis, A.J., Effect of a nonzero temperature on quantum critical points in itinerant fermion systems. *Phys. Rev. B* **48**, 7183-7196 (1993).
- ³ Continentino, M.A., Quantum scaling in many-body systems. *Phys. Rep.* **239**, 179-213 (1994).
- ⁴ Si, Q., Rabello, S., Ingersent, K. & Smith, J.L., Locally critical quantum phase transitions in strongly correlated metals. *Nature* **413**, 804-808 (2001).
- ⁵ Coleman, P. & Pépin, C., What is the fate of the heavy electron at a quantum critical point? *Physica B* **312**, 383-389 (2002).
- ⁶ Gegenwart, P. *et al.*, Magnetic-field induced quantum critical point in YbRh₂Si₂. *Phys. Rev. Lett.* **89**, 056402 (2002).
- ⁷ Heuser, K. *et al.*, Inducement of non-Fermi-liquid behavior with a magnetic field. *Phys. Rev. B* **57**, R4198-201, (1998).
- ⁸ Stockert, O. *et al.*, Pressure versus magnetic-field tuning of a magnetic quantum phase transition. *Physica B* **312-313**, 458-460 (2002).
- ⁹ Trovarelli, O. *et al.*, YbRh₂Si₂: Pronounced non-Fermi-liquid effects above a low-lying magnetic phase transition. *Phys. Rev. Lett.* **85**, 626-629 (2000).
- ¹⁰ Mederle, S. *et al.*, Unconventional metallic state in YbRh₂(Si_{1-x}Ge_x)₂ - a high pressure study. *J. Phys.: Condens. Matter* **14**, 10731-10736 (2002).
- ¹¹ Plessel, J., Hochdruckuntersuchungen an Yb-Kondo-Gitter-Systemen in der Nähe einer magnetischen Instabilität. *Dissertation, Universität zu Köln* (2001).
- ¹² Francois, M., Venturini, G., Marchêché, J.F., Malaman, B. & Roques, B., De Nouvelles séries de germaniures, isotopes de U₄Re₇Si₆, ThCr₂Si₂ et CaBe₂Ge₂, dans les systèmes

- ternaires R–T–Ge où R est un élément des terres rares et T \equiv Ru, Os, Rh, Ir: supraconductivité de LaIr₂Ge₂. *J. Less Common Metals* **113** 231-237 (1985).
- ¹³ Kadowaki, K. & Woods, S.B., Universal relationship of the resistivity and specific heat in heavy-fermion compounds. *Solid State Commun.* **58**, 507-509 (1986).
- ¹⁴ Gegenwart, P. *et al.*, Divergence of the heavy quasiparticle mass at the antiferromagnetic quantum critical point in YbRh₂Si₂. *Acta Phys. Pol. B* **34**, 323-334 (2003).
- ¹⁵ Landau, L.D., The theory of a Fermi liquid. *Sov. Phys. JETP* **3**, 920-925 (1957).
- ¹⁶ Paul, I. & Kotliar, G., Thermoelectric behavior near the magnetic quantum critical point. *Phys. Rev. B* **64**, 184414 (2001).
- ¹⁷ Giamarchi, T. , Varma, C.M., Ruckenstein, A.E. & Nozières, P., Singular low energy properties of an impurity model with finite range interactions. *Phys. Rev. Lett.* **70**, 3967-3970 (1993).
- ¹⁸ Schröder, A. *et al.*, Onset of antiferromagnetism in heavy-fermion metals. *Nature* **407**, 351-355 (2000).
- ¹⁹ Carter, G.C. *et al.*, in Metallic shifts in NMR. *Progress in Materials Science*, **Vol. 20, Part I**, ed. Chalmers, B., Christian, J.W. & Massalski, T.B. (Pergamon Press, Oxford 1977).

Acknowledgements

We would like to acknowledge discussions with J. Ferstl, C. Langhammer, S. Mederle, N. Oeschler, I. Zerec, G. Sparn, O. Stockert, M. Abd-Elmeguid, J. Hopkinson, A. I. Larkin, and I. Paul. Work at Dresden is partially supported by the Fonds der Chemischen Industrie and by the FERLIN project of the European Science Foundation. P. Coleman is supported by the National Science Foundation. Y. Tokiwa is a Young Scientist Research Fellow supported by the Japan Society for the Promotion of Science.

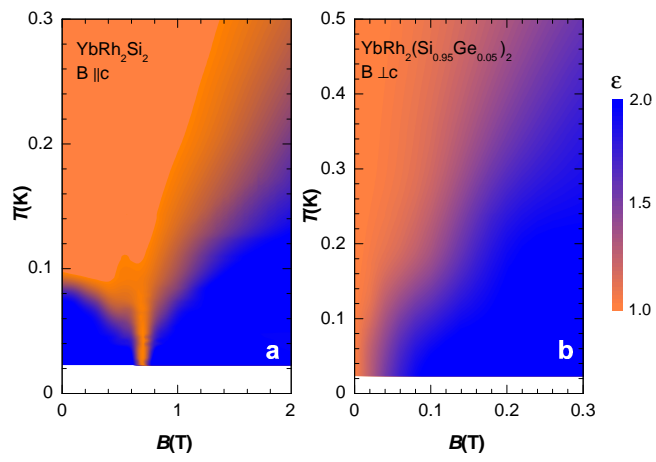


FIG. 1. Evolution of ε , the exponent in $\Delta\rho(T) = [\rho(T) - \rho_o] \propto T^\varepsilon$, within the temperature–field phase diagram of $\text{YbRh}_2(\text{Si}_{1-x}\text{Ge}_x)_2$ single crystals. The non–Fermi–liquid (NFL) behavior, $\varepsilon = 1$ (yellow color), is found to occur at the lowest temperatures right at the quantum critical point (QCP), $B = B_c$ [**a**, $x = 0$, $B_c = 0.66$ T ($\parallel c$), residual resistivity $\rho_o = 1\mu\Omega\text{cm}$; **b**, $x = 0.05$, $B_c = 0.027$ T ($\perp c$), $\rho_o = 5\mu\Omega\text{cm}$] and in a largely extended field range at higher temperatures. For $B > B_c$, a broad cross–over regime from the NFL state to the field–induced heavy Landau Fermi–liquid (LFL) state (at lower temperature) is stated. The LFL state is characterized by $\Delta\rho(T) \propto T^\varepsilon$, $\varepsilon = 2$ (blue color). As shown in (**a**) the antiferromagnetically ordered phase of pure YbRh_2Si_2 below $T_N = 70$ mK and B_c shows, owing to an extremely small ordered moment, the outward appearance of a heavy LFL state, too. Its phase boundary to the paramagnetic state is manifested by a rapid change in ε from 2 to 1.

The low ordering temperature of pure YbRh_2Si_2 increases as external pressure is applied⁹. The extrapolation of $T_N(p) \rightarrow 0$ yields a critical pressure $p_c = -0.3(1)$ GPa, reflecting that a small expansion of the unit cell volume, V , would tune $T_N \rightarrow 0$. This can be achieved by the substitution of Si by the isoelectronic, but larger, Ge¹⁰. Studies of the electrical resistivity under pressure revealed a $T_N \propto (p + p_c)^n$ variation, with $n = 1.33$ for both compounds. The $T_N(p)$ -dependences of the $x = 0$ and $x = 0.05$ crystals can be matched if all $x = 0.05$ data points are shifted by the same amount $\Delta p = -0.17(2)$ GPa to lower pressure¹⁰, yielding $T_N = 20(5)$ mK. Using the bulk modulus $B_0 = 189$ GPa of YbRh_2Si_2 ¹¹, the small pressure shift of $\Delta p = -0.17(2)$ GPa is equivalent to a volume expansion of $\Delta V = 0.14(3)$ Å³. This transforms into an *effective* Ge content $x_{\text{eff}} = 0.019(6)$, if the value $\Delta V/V = 7.65(78)$ % for the relative change of the unit-cell volume with Ge concentration in the solid-solution $\text{YbRh}_2(\text{Si}_{1-x}\text{Ge}_x)_2$ is used, with $V(x = 0) = 158.4(2)$ Å³ and $V(x = 1) = 166.07(54)$ Å³, cf. Ref.¹², in agreement with microprobe analysis¹⁴.

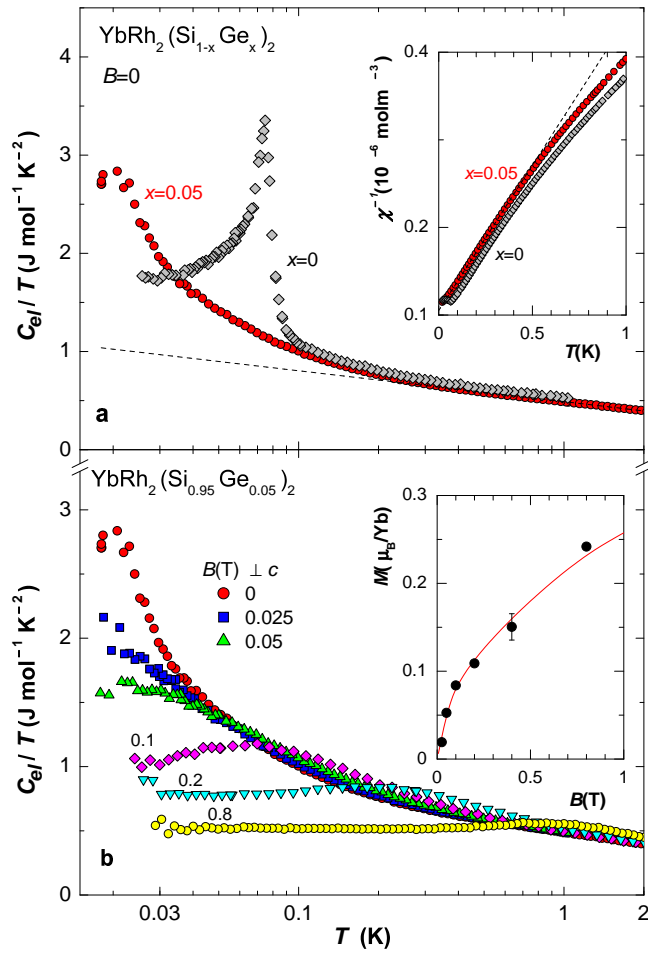


FIG. 2. Low-temperature electronic specific heat of $\text{YbRh}_2(\text{Si}_{1-x}\text{Ge}_x)_2$ single crystals as C_{el}/T vs T in semi-log plots at zero field and at low values of the applied magnetic field B . Insets show low- T $B = 0$ ac-susceptibility as χ^{-1} vs T (**a**) and magnetization as M vs B (**b**). C_{el} is obtained by subtracting the nuclear quadrupolar contribution, $C_{\text{Q}} = \alpha_{\text{Q}}/T^2$ (with $\alpha_{\text{Q}} = 5.68 \times 10^{-6}$ JKmol $^{-1}$, calculated from recent Mössbauer results¹¹) (**a**) and, in addition, the nuclear Zeeman contribution $C_{\text{hf}} = \alpha(B)/T^2$ (**b**), from the raw data. Here, $\alpha(B)$ has been deduced by plotting CT^2 vs T^3 . The magnetization, M vs magnetic field B (black points in the inset), is calculated via $(B_{\text{hf}} - B)/A$, with A the hyperfine coupling constant for Yb in this compound and the hyperfine field $B_{\text{hf}} = \sqrt{(\alpha(B) - \alpha_{\text{Q}})/\alpha_{\text{dip}}}$; α_{dip} represents the strength of the nuclear magnetic dipolar interaction and amounts to 7.58×10^{-8} JKmol $^{-1}\text{T}^{-2}$, Ref.¹⁹. With the assumption of $A = 120$ T/ μ_{B} , the data points agree perfectly with the measured magnetization curve at 40 mK (red line in the inset of **b**).

The $B = 0$ results shown in **(a)** reveal an upturn in $C_{\text{el}}(T)/T$ for paramagnetic $\text{YbRh}_2(\text{Si}_{1-x}\text{Ge}_x)_2$ ($x = 0$, $T_{\text{N}} = 70$ mK; $x = 0.05$, $T_{\text{N}} = 20$ mK) below $T = 0.3$ K. In the same temperature range the susceptibility $\chi(T)$ shows a Curie-Weiss law, $\chi^{-1} \propto (T - \Theta)$ [inset of **(a)**]. For both samples very similar values are found for the Weiss temperature, $\Theta \approx -0.3$ K, as well as for the large effective moment, $\mu_{\text{eff}} \approx 1.4\mu_{\text{B}}/\text{Yb}^{3+}$. For $\text{YbRh}_2(\text{Si}_{0.95}\text{Ge}_{0.05})_2$, entropy is shifted from low to higher temperatures when a magnetic field is applied **(b)**. The cross-over temperature between the field-induced LFL state ($C_{\text{el}}(T)/T \approx \text{const.}$) and the NFL state at higher temperature is depicted by the position of the broad hump in $C_{\text{el}}(T)/T$ which shifts upwards linearly with the field, $B \leq 0.8$ T ($\perp c$).

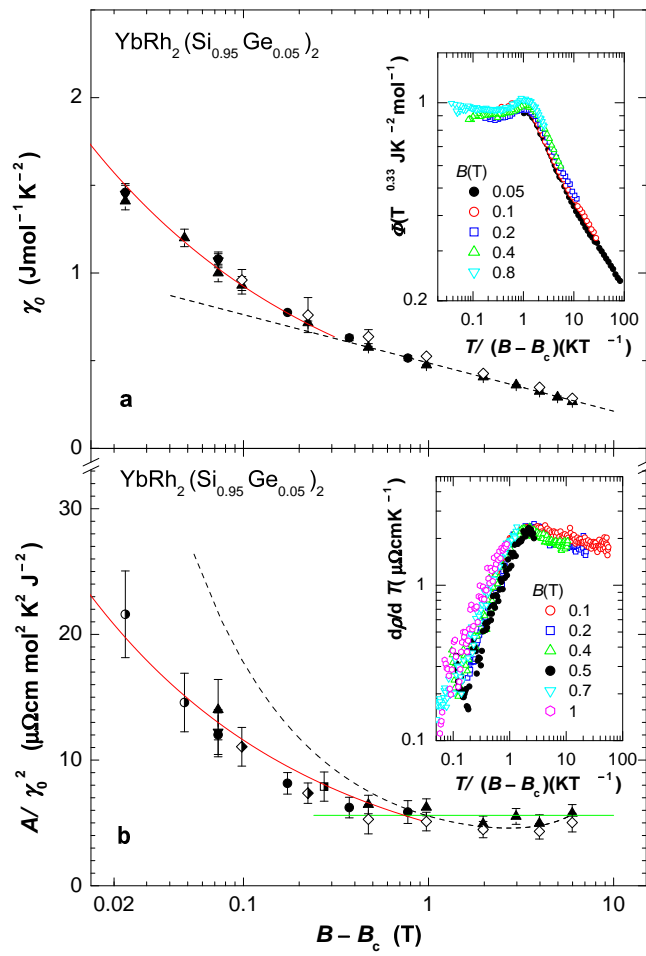


FIG. 3. Field dependences of the Sommerfeld coefficient, γ_o , of the electronic specific heat **(a)** and of the ratio of the A -coefficient in the T^2 term of the electrical resistivity and γ_o^2 **(b)** for $\text{YbRh}_2(\text{Si}_{0.95}\text{Si}_{0.05})_2$. Note that γ_o and A are proportional to the effective quasiparticle mass and the effective quasiparticle-quasiparticle scattering cross section, respectively. The magnetic field was applied perpendicular to the c -axis, and the applied field values are corrected, on the abscissae, by the value of the critical field, $B_c = 0.027$ T. γ_o -values in **(a)** were obtained from two different samples: Three independent measurements on sample #1 are displayed by closed symbols (circles, up and down triangles). The open symbols (diamonds) show the results of measurements on sample #2. As $B \rightarrow B_c$, γ_o diverges $\propto (B - B_c)^{-0.33}$ (red line), i. e., much stronger than logarithmically (black dashed line). The symbols used in the semi-log plot $K = A/\gamma_o^2$ vs $(B - B_c)$ of **(b)** correspond to values for the electronic specific heat coefficient shown in **(a)**. Half filled circles (squares) display data for which the A -coefficient of the electrical resistivity was determined by extrapolating (interpolating) $A(B - B_c)$ with respect to $(B - B_c)$. The half filled diamond represents a point for which the γ_o value was obtained by interpolation. The black dashed line indicates $K_{\text{SDW}} \propto [(B - B_c) \ln^2(B - B_c)]^{-1}$ for the 2D SDW scenario¹⁶. This is at strong variance from the (at $B - B_c < 0.3$ T) experimentally observed $K \propto (B - B_c)^{-1/3}$, arising from the stronger than logarithmic increase of γ_o upon cooling (red line in **a**). For $(B - B_c) > 0.3$ T, K becomes field independent within the error bars at a constant value of $5.4 \mu\Omega\text{cmmol}^2\text{K}^2\text{J}^{-2}$ (green horizontal line in **b**). A similar high field behavior has been reported previously⁶ on pure YbRh_2Si_2 . Noteworthy, an almost identical value for K was found. Insets show scaling behavior of the low- T electronic specific heat where, according to equation (1), the ordinate is displaying $\Phi(B, T) = (B - B_c)^{0.33} C_{\text{el}}/T$, **a**, as well as of the temperature derivative of the electrical resistivity, $d\rho/dT$, **b**, as a function of $T/(B - B_c)$.